

Rapidly rotating pulsar radiation in vacuum nonlinear electrodynamics

V. I. Denisov¹, I. P. Denisova², A. B. Pimenov¹, V. A. Sokolov^{1,a}

¹ Physics Department, Moscow State University, Moscow 119991, Russia

² Moscow Aviation Institute (National Research University), Volokolamskoe Highway 4, Moscow 125993, Russia

Received: 5 September 2016 / Accepted: 23 October 2016 / Published online: 8 November 2016

© The Author(s) 2016. This article is published with open access at Springerlink.com

Abstract In this paper we investigate the corrections of vacuum nonlinear electrodynamics on rapidly rotating pulsar radiation and spin-down in the perturbative QED approach (post-Maxwellian approximation). An analytical expression for the pulsar's radiation intensity has been obtained and analyzed.

1 Introduction

Vacuum nonlinear electrodynamics effects is an object that piques a great interest in contemporary physics [1–4]. First of all it is related to the emerging opportunities of experimental research in terrestrial conditions using extreme laser facilities like extreme light infrastructure (ELI) [5–7], Helmholtz International Beamline for extreme fields (HIBEF) [8]. It opens up new possibilities in fundamental physics tests [9–11] with an extremal electromagnetic field intensities and particle accelerations that have never been obtained before.

At the same time the investigation of the effects of vacuum nonlinear electrodynamics in astrophysics gives us an additional opportunity to carry out versatile research using the natural extreme regimes of strong electromagnetic and gravitational fields with intensities unavailable yet in laboratory conditions. Compact astrophysical objects with a strong field, such as pulsars and magnetars, are best suited for vacuum nonlinear electrodynamics research. Nowadays, there are many effects of vacuum nonlinear electrodynamics predicted in the pulsar's neighborhood. For example vacuum electron–positron pair production [12] and photon splitting [13], photon frequency doubling [14], light by light scattering, and vacuum birefringence [15], transient radiation ray bending [16,17] and normal waves delay [18]. Some of the predicted effects are indirectly confirmed by astrophysical observations. For instance the evidence of the absence of the

high-field (surface fields more than $B_p > 10^{13}G$) radio loud pulsars can be explained by pair-production suppression due to photon splitting [19].

In this paper we calculate vacuum nonlinear electrodynamics corrections to electromagnetic radiation of rapidly rotating pulsar and analyze pulsar spin-down under these corrections.

This paper is organized as follows. In Sect. 2, we present vacuum nonlinear electrodynamics models and discuss their main physical properties and predictions. In Sect. 3 pulsar radiation in post-Maxwellian approximation is calculated. Section 4 is devoted to an analysis of the pulsar's spin-down vacuum nonlinear electrodynamics influence. In the last section we summarize our results.

2 Vacuum nonlinear electrodynamics theoretical models

Modern theoretical models of nonlinear vacuum electrodynamics suppose that the electromagnetic field Lagrange function density $L = L(I_{(2)}, I_{(4)})$ depends on both independent invariants $I_{(2)} = F_{ik}F^{ki}$ and $I_{(4)} = F_{ik}F^{kl}F_{lm}F^{mi}$ of the electromagnetic field tensor F_{ik} . The specific relationship between the Lagrange function and the invariants depends on the choice of the theoretical model. Nowadays the most promising models are Born–Infeld and Heisenberg–Euler electrodynamics.

Born–Infeld electrodynamics is a phenomenological theory originating from the requirement of self-energy finiteness for a point-like electrical charge [20]. In subsequent studies, the attempts of quantization were performed [21,22] and also it was revealed that Born–Infeld theory describes the dynamics of electromagnetic fields on D-branes in string theory [23–25]. As the main features of Born–Infeld electrodynamics one can note the absence of birefringence (however, there are modifications of the Born–Infeld theory [26] with the vacuum birefringence predictions) and dichroism for

^ae-mail: sokolov.sev@inbox.ru

electromagnetic waves propagating in external electromagnetic field [27]. Furthermore, this theory has a distinctive feature – the value of electric field depends on the direction of approach to the point-like charge. This property was noted by the authors of the theory and also eliminated by them in the subsequent model development [28].

Lagrangian function in Born–Infeld electrodynamics has the following form:

$$L = -\frac{1}{4\pi a^2} \left\{ \sqrt{\left[1 - \frac{a^2}{2} I_{(2)} - \frac{a^4}{4} I_{(4)} + \frac{a^4}{8} I_{(2)}^2 \right]} - 1 \right\}, \tag{1}$$

where a is a characteristic constant of theory, the inverse value of which has a meaning of maximum electric field for the point-like charge. For this constant only the following estimation is known: $a^2 < 1.2 \times 10^{-32} \text{ G}^{-2}$.

The other nonlinear vacuum electrodynamics – the Heisenberg–Euler model [15,29] – was derived in quantum field theory and describes one-loop radiative corrections caused by vacuum polarization in a strong electromagnetic field. Unlike the Born–Infeld electrodynamics, this theoretical model possesses vacuum birefringent properties in a strong field.

The effective Lagrangian function for Heisenberg–Euler theory has the following form:

$$L = \frac{I_{(2)}}{16\pi} - \frac{\alpha B_c^2}{8\pi^2} \int_0^\infty \frac{e^{-\sigma} d\sigma}{\sigma^3} \left[xy\sigma^2 \text{ctg}(x\sigma) \text{cth}(y\sigma) + \frac{\sigma^2}{3} (x^2 - y^2) - 1 \right] d\sigma, \tag{2}$$

where $B_c = m^2 c^3 / e\hbar = 4.41 \times 10^{13} \text{ G}$ is the value of the characteristic field in quantum electrodynamics, e and m are the electron charge and mass, $\alpha = e^2 / \hbar c$ is the fine structure constant, and for brevity we use the notations

$$x = -\frac{i}{\sqrt{2}B_c} \left\{ \sqrt{\frac{1}{2}(\mathbf{B}^2 - \mathbf{E}^2) + i(\mathbf{B} \mathbf{E})} - \sqrt{\frac{1}{2}(\mathbf{B}^2 - \mathbf{E}^2) - i(\mathbf{B} \mathbf{E})} \right\}, \tag{3}$$

$$y = \frac{1}{\sqrt{2}B_c} \left\{ \sqrt{\frac{1}{2}(\mathbf{B}^2 - \mathbf{E}^2) + i(\mathbf{B} \mathbf{E})} + \sqrt{\frac{1}{2}(\mathbf{B}^2 - \mathbf{E}^2) - i(\mathbf{B} \mathbf{E})} \right\}. \tag{4}$$

Many attempts to find the experimental status for each of these theories were made a long time ago, but nowadays it still remains ambiguous. There is experimental evidence in favor of each of them. Heisenberg–Euler electrodynamics

predictions were experimentally proved in Delbrück light by light scattering [30], nonlinear Compton scattering [31], Schwinger pair production in multiphoton scattering [1]. At the same time the recent astrophysical observations [32,33] point on the absence of the vacuum birefringence effect which favors the Born–Infeld theory prediction. The measurements performed for the speed of light in vacuum show that it does not depend on wave polarization with the accuracy $\delta c/c < 10^{-28}$. So clarification of the vacuum nonlinear electrodynamics status requires the expansion of the experimental test list both in terrestrial and astrophysical conditions. The main hopes as regards this way to proceed are assigned to the experiments with ultra-high intensity laser facilities [4] and astrophysical experiments with X-ray polarimetry [34] in pulsars and magnetars neighborhood.

As follows from the Lagrangians (1)–(2) vacuum nonlinear electrodynamics’ influence becomes valuable only in strong electromagnetic fields, comparable to $E, B \sim 1/a$ for Born–Infeld theory and $E, B \sim B_c$ for Heisenberg–Euler electrodynamics [35]. In the case of relatively weak fields ($E, B \ll B_c$) the exact expressions (1) and (2) can be decomposed and written [36] in the form of a unified parametric post-Maxwellian Lagrangian:

$$L = \frac{1}{32\pi} \left\{ 2I_{(2)} + \xi \left[(\eta_1 - 2\eta_2) I_{(2)}^2 + 4\eta_2 I_{(4)} \right] \right\}, \tag{5}$$

where $\xi = 1/B_c^2 = 0.5 \times 10^{-27} \text{ G}^{-2}$, and the post-Maxwellian parameters η_1 and η_2 depend on the choice of the theoretical model. In the case of Heisenberg–Euler electrodynamics the post-Maxwellian parameters η_1 and η_2 are coupled to the fine structure constant α [37]:

$$\eta_1 = \frac{\alpha}{45\pi} = 5.1 \times 10^{-5}, \quad \eta_2 = \frac{7\alpha}{180\pi} = 9.0 \times 10^{-5}. \tag{6}$$

For Born–Infeld electrodynamics these parameters are equal to each other and they can be expressed through the field induction $1/a$ typical of this theory [37]:

$$\eta_1 = \eta_2 = \frac{a^2 B_c^2}{4} < 4.9 \times 10^{-6}. \tag{7}$$

The electromagnetic field equations for the post-Maxwellian vacuum electrodynamics with the Lagrangian (5) are equivalent [35] to the equations of Maxwell electrodynamics of continuous media,

$$\partial_m F_{ik} + \partial_i F_{km} + \partial_k F_{mi} = 0, \tag{8}$$

$$\frac{\partial Q^{ki}}{\partial x^i} = -\frac{4\pi}{c} j^k, \tag{9}$$

with the specific nonlinear constitutive relations [18]

$$Q^{ki} = F^{ki} + \xi \left[(\eta_1 - 2\eta_2) I_{(2)} F^{ki} + 4\eta_2 F_{(3)}^{ki} \right], \tag{10}$$

where $F_{(3)}^{ki} = F^{kn} F_{nm} F^{mi}$ is the third power of the electromagnetic field tensor. The tensor Q^{ik} can be separated into two terms $Q^{ki} = F^{ki} + M^{ki}$, one of which, M^{ki} , will have a meaning similar to the matter polarization tensor in electrodynamics of continuous media.

Also it should be noted that in a post-Maxwellian approximation the stress-energy tensor T^{ik} and Poynting vector S have the form

$$T^{ik} = \frac{1}{4\pi} \left\{ (1 + \xi\eta_1 I_{(2)}) F_{(2)}^{ik} - \frac{g^{ik}}{8} \left[2I_{(2)} + \xi(\eta_1 + 2\eta_2) I_{(2)}^2 - 4\eta_2 \xi I_{(4)} \right] \right\}, \tag{11}$$

$$S^\mu = cT^{0\mu} = \frac{c}{4\pi} \left[1 + \xi\eta_1 I_{(2)} \right] F_{(2)}^{0\mu}, \tag{12}$$

where $F_{(2)}^{ik} = g^{ni} F_{nm} F^{mk}$ is the second power of the electromagnetic field tensor, g^{ik} is the metric tensor; and the Greek index takes the value $\mu = 1, 2, 3$.

As was shown in [38], post-Maxwellian approximation turns out to be very convenient for vacuum nonlinear electrodynamics analysis, so we will use this representation (8)–(12) to calculate the radiation of the rapidly rotating pulsar.

3 Rapidly rotating pulsar radiation in post-Maxwellian nonlinear electrodynamics

Pulsars are the compact objects best suited for vacuum nonlinear electrodynamics tests in astrophysics. They possess sufficiently strong magnetic fields with the strength varying from $B_p \sim 10^9 G$ up to $B_p \sim 10^{14} G$; as these values are close to B_c the vacuum nonlinear electrodynamics' influence can be manifested. At the same time, the pulsar's fast rotation may enhance the nonlinear influence on its radiation.

Let us consider a pulsar of radius R_s , rotating around an axis passing through its center with the angular velocity ω . We shall suppose that the rotation is fast enough, so the linear velocity for the points on the pulsar's surface is comparable to the speed of light $\omega R_s/c \sim 1$. We assume that the pulsar's magnetic dipole moment \mathbf{m} is inclined to the rotation axis at the angle θ_0 , therefore the cartesian coordinates of this vector vary under rotation as $\mathbf{m} = \{m_x = m \sin \theta_0 \cos \omega t, m_y = m \sin \theta_0 \sin \omega t, m_z = m \cos \theta_0\}$.

As the vacuum nonlinear electrodynamics' influence in post-Maxwellian approximation has the character of a small correction to Maxwell theory one can represent the total electromagnetic field tensor F^{ki} in the form

$$F^{ki} = F_{(0)}^{ki} + f^{ki}, \tag{13}$$

where $F_{(0)}^{ki}$ is the electromagnetic field tensor of the rotating magnetic dipole \mathbf{m} in Maxwell electrodynamics and f^{ik} is the vacuum nonlinear correction. Substituting (13) into (10) and retaining only the terms linear in a small value f^{ik} it can be found that

$$Q^{ik} \simeq f^{ik} + F_{(0)}^{ik} + M_{(0)}^{ik}, \tag{14}$$

where $M_{(0)}^{ik} = M^{ik}(F_{(0)}^{nj})$ is the polarization tensor calculated in the approximation of the Maxwell electrodynamics field $F_{(0)}^{nj}$. The electromagnetic field equations (8)–(9) with account of (13)–(14) then will take the form

$$\begin{aligned} \partial_m F_{ik}^{(0)} + \partial_i F_{km}^{(0)} + \partial_k F_{mi}^{(0)} + \partial_m f_{ik} + \partial_i f_{km} + \partial_k f_{mi} &= 0, \\ \frac{\partial f^{ki}}{\partial x^i} + \frac{\partial F_{(0)}^{ki}}{\partial x^i} + \frac{\partial M_{(0)}^{ki}}{\partial x^i} &= -\frac{4\pi}{c} j^k. \end{aligned} \tag{15}$$

The solution of these equations may be obtained by the successive approximation method. In the initial approximation we assume that $F_{mi}^{(0)}$ is the solution of the Maxwell electrodynamics equations

$$\begin{aligned} \partial_m F_{ik}^{(0)} + \partial_i F_{km}^{(0)} + \partial_k F_{mi}^{(0)} &= 0, \\ \frac{\partial F_{(0)}^{ki}}{\partial x^i} &= -\frac{4\pi}{c} j^k, \end{aligned} \tag{16}$$

corresponding to rotating magnetic dipole \mathbf{m} and a current density which by j^k is represented in the right hand side of these equations. In this case, from (15) it follows that the vacuum nonlinear electrodynamics' corrections f_{ik} may be obtained as a solution of linearized equations:

$$\begin{aligned} \partial_m f_{ik} + \partial_i f_{km} + \partial_k f_{mi} &= 0, \\ \frac{\partial f^{ki}}{\partial x^i} + \frac{\partial M_{(0)}^{ki}}{\partial x^i} &= 0. \end{aligned} \tag{17}$$

To satisfy the homogeneous equation (17) electromagnetic potential A^k should be introduced $f_{ik} = \partial_k A_i - \partial_i A_k$. Using this potential the inhomogeneous equation (18) under the Lorentz gauge will take the form

$$\partial_n \partial^n A^k = \frac{\partial M_{(0)}^{ki}}{\partial x^i}. \tag{19}$$

It is more convenient to rewrite the last equation in terms of the antisymmetric Hertz tensor Π^{ki} defined by

$$A^k = -\frac{\partial \Pi^{ki}}{\partial x^i}. \tag{20}$$

In this case Eq. (19) will take the simple form

$$-\partial_n \partial^n \Pi^{ki} = \square \Pi^{ki} = M_{(0)}^{ki}, \tag{21}$$

where $\square = -\partial_n \partial^n$ is the D'Alembert operator. Six independent equations in (21) may be expressed in vector form by introducing the Hertz electric $\mathbf{\Pi}$ and magnetic \mathbf{Z} potentials [39]:

$$\mathbf{\Pi}^\alpha = \Pi^{\alpha 0}, \quad \mathbf{Z}^\alpha = \frac{1}{2} \epsilon^{\alpha\mu\nu} \Pi_{\mu\nu}, \tag{22}$$

where $\epsilon^{\alpha\mu\nu}$ is the Levi-Civita symbol and all of the indices take values $\alpha, \mu, \nu = 1, 2, 3$. In terms of these potentials Eq. (21) can be rewritten

$$\square \mathbf{\Pi} = \mathbf{P}_0, \quad \square \mathbf{Z} = \mathbf{M}_0, \tag{23}$$

where the source vectors \mathbf{P}_0 and \mathbf{M}_0 are expressed from polarization tensor $M_{ik}^{(0)}$ by the equalities

$$\mathbf{P}_0^\alpha = M_{(0)}^{\alpha 0}, \quad \mathbf{M}_0^\alpha = \frac{1}{2} \epsilon^{\alpha\mu\nu} M_{\mu\nu}^{(0)}. \tag{24}$$

The explicit components of these vectors may easily be obtained in Minkowski space-time with the use of (10) and (24):

$$\mathbf{P}_0 = 2\xi \{ \eta_1 (\mathbf{E}_0^2 - \mathbf{B}_0^2) \mathbf{E}_0 + 2\eta_2 (\mathbf{B}_0 \mathbf{E}_0) \mathbf{B}_0 \}, \tag{25}$$

$$\mathbf{M}_0 = 2\xi \{ \eta_1 (\mathbf{E}_0^2 - \mathbf{B}_0^2) \mathbf{B}_0 - 2\eta_2 (\mathbf{B}_0 \mathbf{E}_0) \mathbf{E}_0 \}, \tag{26}$$

where \mathbf{E}_0 and \mathbf{B}_0 are the electromagnetic field components of the rotating magnetic dipole in Maxwell electrodynamics, the expressions for which are well described in the literature [40] and the field vectors themselves have the form

$$\mathbf{B}_0(\mathbf{r}, t) = \frac{3(\mathbf{m}(\tau) \mathbf{r}) \mathbf{r} - r^2 \mathbf{m}(\tau)}{r^5} - \frac{\dot{\mathbf{m}}(\tau)}{cr^2} + \frac{3(\dot{\mathbf{m}}(\tau) \mathbf{r}) \mathbf{r}}{cr^4} + \frac{(\ddot{\mathbf{m}}(\tau) \mathbf{r}) \mathbf{r} - r^2 \ddot{\mathbf{m}}(\tau)}{c^2 r^3}, \tag{27}$$

$$\mathbf{E}_0(\mathbf{r}, t) = \frac{[\mathbf{r}, \dot{\mathbf{m}}(\tau)]}{cr^3} + \frac{[\mathbf{r}, \ddot{\mathbf{m}}(\tau)]}{c^2 r^2}, \tag{28}$$

where $\tau = t - r/c$ is the retarded time and the dot corresponds to the derivative of the magnetic dipole moment $\mathbf{m}(\tau)$ with respect to the retarded time τ . Therefore, the right hand side of Eq. (23) can be obtained by using of (25)–(28). Equations (23) themselves are the inhomogeneous hyperbolic equations the exact solution methods of which are well developed and described in the literature [41–43]. Since we are interested only in the radiative solutions for the pulsar's field, when solving Eq. (23) one should retain only the terms decreasing not faster than $\sim 1/r$ with the distance to the pulsar. At the same time there are no restrictions on the rotational velocity so $\omega R_s/c \sim 1$. Due to the excessive unwieldiness here we will not represent the whole solutions for the Hertz potentials $\mathbf{\Pi}$ and \mathbf{Z} , but we will use the results for them to

find the components of the electromagnetic field tensor f_{ik} and radiation properties such as the Poynting vector \mathbf{S} and the total intensity I . The Poynting vector components represented by (12) in post-Maxwellian electrodynamics can be simplified by the radiative asymptotic condition $S^\mu \sim 1/r^2$, which actually means that for the radiation description we can use the Maxwellian expression for this vector:

$$S^\mu = c T^{0\mu} \sim \frac{c}{4\pi} F_{(2)}^{0\mu}. \tag{29}$$

Finally, the total intensity can be obtained by integrating of the Poynting vector by the surface with the normal \mathbf{n} directed to the observer located at the large distance $r \gg R_s$ from the pulsar:

$$I = \int (\mathbf{S} \mathbf{n}) r^2 d\Omega, \tag{30}$$

where $d\Omega$ is the solid angle.

Solutions of Eq. (23) with the right hand side (25), (26) lead to the following expression for the pulsar radiation intensity:

$$\begin{aligned} I = & \frac{2\omega^4 B_p^2 R_s^6}{3c^3} \sin^2 \theta_0 \left\{ 1 + \frac{2}{35Y^3} \frac{B_p^2}{B_c^2} \left(24Y^9 \left[\frac{1}{15} \eta_1 - \eta_2 \right] \right. \right. \\ & \times Ci(2Y) \sin^2 \theta_0 + 4Y^9 \left[\eta_2 - \frac{311}{45} \eta_1 \right] Ci(2Y) \\ & + Y^3 \left[\frac{\eta_1 - 15\eta_2}{5} (2Y^4 - 3Y^2) \right. \\ & \left. \left. - 18\eta_1 - 10\eta_2 \right] \cos(2Y) \sin^2 \theta_0 \right. \\ & + \frac{Y}{6} \left[\frac{45\eta_2 - 311\eta_1}{15} (2Y^6 - 3Y^4) + (172\eta_1 - 60\eta_2) Y^2 \right. \\ & \left. \left. - 336\eta_1 \right] \cos(2Y) + Y^2 \left[\frac{30\eta_2 - 2\eta_1}{5} (2Y^6 - Y^4) \right. \right. \\ & \left. \left. - \frac{41\eta_1 + 85\eta_2}{5} Y^2 + 9\eta_1 + 5\eta_2 \right] \sin(2Y) \sin^2 \theta_0 \right. \\ & + \frac{1}{3} \left[\frac{311\eta_1 - 45\eta_2}{15} (2Y^8 - Y^6 + 3Y^4) \right. \\ & \left. \left. + (15\eta_2 - 141\eta_1) Y^2 + 84\eta_1 \right] \sin(2Y) \right\}, \tag{31} \end{aligned}$$

where the following notations are used for brevity: $k = \omega/c$ and $Y = k R_s$, also B_p is the surface magnetic field inductance and $Ci(x) = \int_\infty^x \frac{\cos u}{u} du$ is an integral cosine.

It is obvious that the intensity obtained can be represented in a form which distinguishes the Maxwell radiation intensity and the vacuum nonlinear electrodynamics correction. In this representation it is convenient to introduce the ‘‘correction function’’ $\Phi(\theta_0, Y)$, which is a multiplier before the scaling factor B_p^2/B_c^2 determining how strong the vacuum nonlinear

electrodynamics' influence on the pulsar radiation is,

$$I = \frac{2\omega^4 B_p^2 R_s^6}{3c^3} \sin^2 \theta_0 \left\{ 1 + \frac{B_p^2}{B_c^2} \Phi(\theta_0, Y) \right\}. \quad (32)$$

For most known rapidly rotating pulsars [44] with $Y \sim 1$ the factor $B_p^2/B_c^2 \ll 1$ is small, which matches the requirements of the post-Maxwellian approximation. At the same time this means that the vacuum nonlinear electro-dynamics corrections will be sufficiently suppressed in comparison with the Maxwell electro-dynamics radiation. However, this assessment may be waived for special sources of so-called fast radio bursts (FRB's), six cases of which have recently been discovered [46]. One of the hypotheses explaining the nature of FRBs assumes that their source is a rapidly rotating neutron star with the strong surface magnetic field $B_p > B_c$ called blitzar [45]. In this case vacuum nonlinear electro-dynamics corrections to the pulsar radiation became significant but at the same time this makes a strict solution (31) inapplicable because it was obtained in the low-field limit. So our further evaluations will be applied to the case of the typical rapidly rotating pulsar, for instance PSR B1937+21 with $B_p \sim 4.2 \times 10^8 G \ll B_c$, and maybe for blitzars but with the restriction $B_p < B_c$. The main purpose of our analysis will be the identification of new qualitative features of the pulsar radiation and comparing vacuum nonlinear corrections to the electromagnetic radiation with the other weak energy loss mechanisms.

Let us investigate the properties of the correction function $\Phi(\theta_0, Y)$. First of all, it should be noted that there is no radiation when the pulsar dipole moment is coaxial with the rotation axis i.e. when θ_0 is zero. The correction function depends both on the angle θ_0 and the angular velocity through $Y = \omega R_s/c$, so $\Phi(\theta_0, Y)$ may be represented as a surface defined in the region where its coordinates take values $0 \leq Y < 1$ and $0 \leq \theta_0 \leq \pi/2$. Some isolines – the relations $\theta_0(Y)$ at which this surface takes a constant value, $\Phi(\theta_0, Y) = \text{const}$ – are represented in the Fig. 1, the numerical values for which were obtained with the η_1 and η_2 from the Heisenberg–Euler theory.

The obtained isolines differ from each other by the absolute value of the correction function but all of them have a pronounced extremum at some point which lies on the red line. This means that for each fixed angle θ_0 between the pulsar dipole moment and the rotation axis there is an angular velocity at which the vacuum nonlinear electro-dynamics corrections become the most pronounced. Increasing Y at constant θ_0 up to the value marked by the red line increases the correction of vacuum nonlinear electro-dynamics. The subsequent Y and angular velocity increase become ineffective because the vacuum corrections in this case will be reduced. It should be noted that increasing $Y \rightarrow 1$ also will enhance

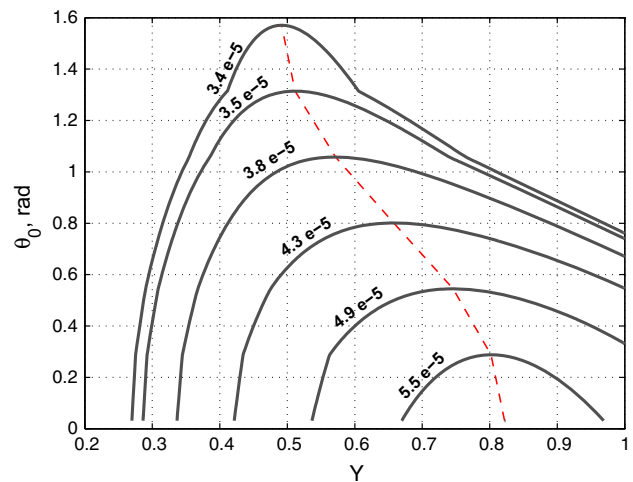


Fig. 1 Correction function isolines and the best contrast line

the total pulsar luminosity, which is $I \propto \omega^4 \sin^2 \theta_0$, but at the same time, as mentioned, this will decrease the vacuum nonlinear electro-dynamics correction on the Maxwell radiation background. For instance, if $\theta_0 \sim \pi/2$ the correction will most significantly stand out for the pulsars with $Y \sim 0.5$. So the correction function $\Phi(\theta_0, Y)$ plays the role of a contrast. And the red line in Fig. 1 marks the relation between θ_0 and Y for the best contrast.

Another distinctive feature of the pulsar radiation is manifested in a sophisticated, non-polynomial dependence between the radiation intensity (31) and the angular velocity, which greatly complicates the analysis. Performing a power-law approximation of (31) will allow us to describe the vacuum nonlinear electro-dynamics' influence on the pulsar spin-down, in traditional terms of braking-indices and torque-functions [47]. It also provides a possibility for comparison of the pulsar spin-down caused by different non-electromagnetic dissipative factors with the power-law relation between the radiation intensity and angular velocity, for instance with the quadrupole gravitational radiation. Let us investigate the features of the pulsar spin-down as a result of the radiation, with the amendments of vacuum nonlinear electro-dynamics.

4 Pulsar spin-down

The observed spin-down rate [47] can be expressed by the derivative of the angular velocity as

$$\dot{\omega} = -\frac{I}{J\omega} = -\frac{2B_p^2 R_s^3}{3J} \sin^2 \theta_0 \left\{ Y^3 + \frac{B_p^2}{B_c^2} Y^3 \Phi \right\}, \quad (33)$$

where J is the pulsar's inertia momentum and the dot means the time derivative. For a description in terms of torque func-

Table 1 Expansion coefficients

θ_0	$\alpha_7 \times 10^4$	$\alpha_6 \times 10^4$	$\alpha_5 \times 10^4$	$\alpha_4 \times 10^4$	$\alpha_3 \times 10^4$
$\pi/2$	1.7	-4.0	2.4	-0.3	-0.2
$\pi/3$	1.5	-3.8	2.7	-0.5	-0.3
$\pi/6$	1.1	-3.6	3.3	-0.9	-0.5

tions, the right hand side of Eq. (33) should be represented in a polynomial form of the angular velocity,

$$Y^3 \Phi(\theta_0, Y) = \sum_n^N \alpha_n(\theta_0) Y^n = \sum_n^N \alpha_n(\theta_0) \left(\frac{\omega R_s}{c}\right)^n, \quad (34)$$

where α_n are decomposition coefficients and the number of the terms N should be selected sufficient to ensure the required accuracy of the decomposition. We will take the number of terms in the expansion (34) equal to $N = 8$. This choice ensures the accuracy of a power-law approximation for the pulsars with $Y > 0.6$ better than 0.1%. It should be noted that the series does not converge at $Y \sim 1$ but its replacement by the partial sum with the specially selected number of terms allows one to accomplish the polynomial approximation, which provides a good match with the exact expression near $Y \sim 1$ but leads to significant errors when $Y \ll 1$. In this case the expansion coefficients (with the η_1 and η_2 from the Heisenberg–Euler theory) for the terms providing the largest contribution are represented in Table 1. The coefficients not listed in the table are small and can be neglected in further consideration.

For quantitative analysis, we will take the inclination angle equal to $\theta_0 = \pi/2$. This choice is justified because it provides the greatest total intensity of the pulsar radiation and in our comparison of nonlinear electrodynamics spin-down with the other non-electrodynamical dissipative factors, it gives the upper limit of the nonlinear electrodynamics’ influence.

After the expansion, the right hand side of the spin-down equation (33) will take the form

$$\dot{\omega} = K_M + \sum_n K_n \omega^n, \quad (35)$$

where K_M corresponds to the torque function of the dipole magnetic radiation in Maxwell electrodynamics [48, 49]:

$$K_M = -\frac{2B_p^2 R_s^6}{3Jc^3} \sin^2 \theta_0, \quad (36)$$

and K_n are the torques originating from the nonlinear vacuum electrodynamics:

$$K_n = \alpha_n(\theta_0) K_M \left(\frac{B_p}{B_c}\right)^2 \left(\frac{R_s}{c}\right)^{n-3}. \quad (37)$$

Let us compare the pulsar spin-down caused by nonlinear vacuum electrodynamics and dissipation caused by gravitational waves radiation. Among several possible ways of gravitational radiation by an isolated pulsar we will choose the two most relevant scenarios – quadrupole mass radiation [50] and the radiation caused by Rossby waves [51], called r-modes.

Quadrupole gravitational radiation may originate by the strain caused by the pulsar rotation, which is especially likely for rapidly rotating pulsars. The spin-down under this kind of radiation can be represented by

$$\dot{\omega} = K_Q \omega^5 = -\frac{32 G J \varepsilon^2}{5 c^5} \omega^5, \quad (38)$$

where G is a gravitational constant and ε is the pulsar ellipticity, which is in accordance with modern representations $\varepsilon < 10^{-4}$ [47].

Another reason for gravitational wave emission by an isolated pulsar are the oscillations modes induced by the pulsar rotation. Gravitational radiation is caused by the instability of such oscillations. As was shown by Owen et al. [52] for young rapidly rotating pulsars, spin-down caused by r-modes can be expressed in the form

$$\dot{\omega} = K_R \omega^7 = -\frac{2^{17} \pi F^2 G M^2 R_s^6 \beta_{\text{sat}}^2}{3^7 5^2 J c^7} \omega^7, \quad (39)$$

where M and R_s are the pulsar mass and its radius, the r-mode oscillations saturation amplitude $10^{-7} \leq \beta_{\text{sat}} \leq 10^{-5}$ was defined by [53], and the dimensionless constant F as has been shown in [54] is to be strictly bounded within $1/(20\pi) \leq F \leq 3/(28\pi)$.

So the torque function for the quadrupole gravitational radiation K_Q can be compared with the nonlinear electrodynamics torque K_5 and the r-mode radiation torque K_R can be compared with the torque K_7 . For this comparison we suppose the pulsar with the typical radius $R_s = 30$ km, mass $M = 2M_\odot$ and inertia momentum $J = 10^{45}$ g cm². Also we assume that the dipole moment inclination is $\theta_0 = \pi/2$ and the post-Maxwellian parameters correspond to Heisenberg–Euler theory (the choice of Born–Infeld parameters in first estimation gives a similar order).

For the pulsar with the surface magnetic field $B_p \sim 10^{11}$ G, for which ellipticity reaches the maximum value $\varepsilon \sim 10^{-4}$, the r-mode saturation amplitude $\beta_{\text{sat}} \sim 10^{-6}$ and $F = 1/(20\pi)$, and we have the following estimation: $K_5/K_Q \sim 1.3 \times 10^{-11}$ and $K_7/K_R \sim 2.6 \times 10^{-7}$. So the quadrupole and r-mode gravitational radiation torque will significantly exceed the nonlinear electrodynamics torque coupled with the terms $\sim \omega^5$ and $\sim \omega^7$ in the spin-down equation. For another parameter set the opposite case takes place. If the pulsar distortion and ellipticity is two orders of magnitude lower ($\varepsilon \sim 10^{-6}$), and the pulsar field is stronger

$B_p \sim 10^{13} G$ than $K_5/K_Q \sim 12.6$ and $K_7/K_R \sim 25.6$. However, it should be noted that rapidly rotating pulsars with such a strong field have not been observed yet. Nevertheless, the theoretical models assuming the blitzars as the sources of fast radio bursts [45] do not eliminate the possibility of such strong electromagnetic fields for the rapidly rotating pulsar. Therefore the obtained ratio between the torques seems very exotic but still cannot be completely discarded.

5 Conclusion

In this work, we have studied the vacuum nonlinear electrodynamics' influence on rapidly rotating pulsar radiation in parameterized post-Maxwellian electrodynamics. Under the assumption of a flat space-time the analytical description of radiation intensity (31) was obtained. Despite the fact that the expression for the intensity is quite complicated for an analysis some new features of pulsar's radiation have been obtained. For instance, it was shown that for the rapidly rotating pulsar vacuum nonlinear electrodynamics' corrections observation is optimal only for certain relations between the inclination angle θ_0 of the magnetic dipole moment to the rotation axis and the angular velocity ω . Such a relation plays the role of a contrast for nonlinear corrections on the total pulsar radiation background. It follows that enhancing of the vacuum nonlinear electrodynamics' influence on pulsar radiation requires not only an increasing magnetic field, but one also needs compliance of conditions marked on Fig. 1 to ensure the best possible contrast for the nonlinear corrections.

The obtained radiation intensity was used to estimate the pulsar spin-down. In this framework, for a description in terms of the torque functions the power-low expansion of the intensity (31) was carried out (35)–(37) with the decomposition coefficients listed in Table 1. This provided an opportunity to compare the nonlinear electrodynamics torque with the weak mechanisms of the energy dissipation, for instance with gravitational wave radiation. For such a comparison the most realistic scenarios of gravitational radiation by isolated pulsars were selected – quadrupole gravitational radiation and r-mode radiation. The quantitative comparison has shown that, for the common rapidly rotating pulsar, gravitational radiation torques significantly exceed the nonlinear electrodynamics torques coupled with the terms of the same ω powers in the spin-down equation. This result can be explained by the low surface magnetic field $B_s < 10^{11} G$ specific for most of the rapidly rotating pulsars' population. The implementation of similar estimates for the compact object possessing a stronger magnetic field (hypothetical blitzar) $B_s \sim 10^{13} G$ shows the possibility of the opposite case when the vacuum nonlinear electrodynamics' torques exceed the

gravitational torque and play a more significant role in the spin-down equation under certain conditions.

Open Access This article is distributed under the terms of the Creative Commons Attribution 4.0 International License (<http://creativecommons.org/licenses/by/4.0/>), which permits unrestricted use, distribution, and reproduction in any medium, provided you give appropriate credit to the original author(s) and the source, provide a link to the Creative Commons license, and indicate if changes were made. Funded by SCOAP³.

References

1. D.L. Burke et al., Phys. Rev. Lett. **79**, 1626 (1997)
2. V.I. Denisov, I.P. Denisova, S.I. Svertilov, Theor. Math. Phys. **135**, 720 (2003)
3. G.O. Schellstede, V. Perlick, C. Lämmerzahl, Phys. Rev. D **92**, 025039 (2015)
4. F.D. Valle et al., Eur. Phys. J. C **76**, 24 (2016)
5. G.V. Dunne, Eur. Phys. J. D **55**, 327 (2009)
6. <http://www.eli-beams.eu/>
7. G. Mourou, T. Tajima, Opt. Photonics News **22**, 47 (2011)
8. <http://www.hzdr.de/db/Cms?pOid=35325&pNid=3214>
9. V.I. Denisov, I.P. Denisova, Opt. Spectrosc. **90**, 928 (2001)
10. A. Paredes, D. Novoa, D. Tommasini, Phys. Rev. Lett. **109**, 253903 (2012)
11. V.I. Denisov, I.P. Denisova, Theor. Math. Phys. **129**, 1421 (2001)
12. J. Schwinger, Phys. Rev. **82**, 664 (1951)
13. S.L. Adler, Ann. Phys. **67**, 599 (1971)
14. P.A. Vshivtseva, V.I. Denisov, I.P. Denisova, Dokl. Phys. **47**, 798 (2002)
15. V.B. Berestetskii, L.P. Pitaevskii, E.M. Lifshitz, *Quantum Electrodynamics* (Pergamon Press, Oxford, UK, 1982)
16. V.I. Denisov, I.P. Denisova, S.I. Svertilov, Dokl. Phys. **46**, 705 (2001)
17. J.Y. Kim, J. Cosmol. Astropart. Phys. **10**, 056 (2011)
18. V.I. Denisov, Theor. Math. Phys. **132**, 1071 (2002)
19. M.G. Baring, A.K. Harding, ApJ **547**, 929 (2001)
20. M. Born, L. Infeld, Proc. R. Soc. **A144**, 425 (1934)
21. M. Born, L. Infeld, Proc. R. Soc. **A147**, 522 (1934)
22. J.B. Kogut, D.K. Sinclair, Phys. Rev. D **73**, 114508 (2006)
23. E.S. Fradkin, A.A. Tseytlin, Phys. Lett. B **163**, 123 (1985)
24. S. Cecotti, S. Ferrara, Phys. Lett. B **187**, 335 (1987)
25. B. Zwiebach, *A First Course in String Theory* (Cambridge University Press, 2004)
26. P. Gaete, J. Helayë-Neto, Eur. Phys. J. C **74**, 3182 (2014)
27. Z. Bilanicka, I. Bialynicki-Birula, Phys. Rev. D **2**, 2341 (1970)
28. B. Hoffmann, L. Infeld, Phys. Rev. **51**, 765 (1937)
29. W. Heisenberg, H. Euler, Z. Phys. **26**, 714 (1936)
30. R.R. Wilson, Phys. Rev. **90**, 720 (1953)
31. C. Bula et al., Phys. Rev. Lett. **76**, 3116 (1996)
32. W.-T. Ni, Phys. Lett. A **379**, 1297 (2015)
33. W.-T. Ni, H.-H. Mei, W. Shan-Jyun, Mod. Phys. Lett. A **28**, 1340013 (2013)
34. P. Soffitta et al., Exp. Astron. **36**, 523 (2013)
35. V.R. Khalilov, *Electrons in Strong Electromagnetic Fields: An Advanced Classical and Quantum Treatment* (Gordon and Breach Science Pub New York, Netherlands, 1996)
36. V.I. Denisov, I.P. Denisova, Dokl. Phys. **46**, 377 (2001)
37. V.I. Denisov, I.P. Denisova, Opt. Spectrosc. **90**, 282 (2001)
38. V.I. Denisov, V.A. Sokolov, M.I. Vasili'ev, Phys. Rev. D **90**, 023011 (2014)

39. I.P. Denisova, M. Dalal, *J. Math. Phys.* **38**, 5820 (1997)
40. V.I. Denisov, I.P. Denisova, V.A. Sokolov, *Theor. Math. Phys.* **172**, 1321 (2012)
41. J. Mathews, R.L. Walker, *Mathematical methods of physics*, 2nd edn. (W. A. Benjamin, New York, 1970)
42. K.V. Zhukovski, *Mosc. Univ. Phys. Bull.* **70**, 93 (2015)
43. K.V. Zhukovski, *Mosc. Univ. Phys. Bull.* **71**, 237 (2016)
44. R.N. Manchester et al., *ATNF pulsar catalog* (Manchester, 2005)
45. H. Falcke, L. Rezzolla, *Astron. Astrophys.* **562**, A137 (2014)
46. A. Loeb, Y. Shvartzvald, D. Maoz, *MNRASL* **439**, L46 (2014)
47. C. Palomba, *Astron. Astrophys.* **354**, 163 (2000)
48. J.P. Ostriker, J.E. Gunn, *ApJ* **157**, 1395 (1969)
49. R.N. Manchester, J.H. Taylor, *Pulsars* (W. H. Freeman, San Francisco, 1977)
50. L.D. Landau, E.M. Lifshitz, *The Classical Theory of Fields*, vol. 2, 4th edn. (Butterworth-Heinemann, 1975)
51. N. Stergioulas, J.A. Font, *Phys. Rev. Lett.* **86**, 1148 (2001)
52. B.J. Owen et al., *Phys. Rev. D* **58**, 084020 (1998)
53. M.G. Alford, K. Schwenzer, *MNRAS* **446**, 3631–3641 (2015)
54. M.G. Alford, K. Schwenzer, *ApJ* **26**, 781 (2014)